

Charge Dynamics in the Colossal Magneto-Resistance Pyrochlore $\text{Tl}_2\text{Mn}_2\text{O}_7$

H. Okamura, T. Koretsune, M. Matsunami, S. Kimura, T. Nanba

Physics Department and Graduate School of Science and Technology, Kobe University, Kobe 657-8501, Japan

H. Imai, Y. Shimakawa, Y. Kubo

Fundamental Research Laboratories, NEC Corporation, Tsukuba 305-8501, Japan

(December 2, 2024)

Optical conductivity data [$\sigma(\omega)$] of the colossal magneto-resistance (CMR) pyrochlore $\text{Tl}_2\text{Mn}_2\text{O}_7$ are presented as functions of temperature (T) and external magnetic field (B). Upon cooling and upon applying B near the Curie temperature, where the CMR manifests itself, $\sigma(\omega)$ shows a clear transition from an insulatorlike to a metallic electronic structure as evidenced by the emergence of a pronounced Drude-like component below ~ 0.2 eV. Analyses on the $\sigma(\omega)$ spectra show that both T - and B -induced evolutions of the electronic structure are very similar to each other, and that they are universally related to the development of macroscopic magnetization. The observed spectral evolutions for $\text{Tl}_2\text{Mn}_2\text{O}_7$ are qualitatively very different from those for the perovskite CMR manganites, which highlights different CMR mechanisms in these compounds.

PACS numbers: 75.30.Vn, 78.30.-j, 78.20.-e

Physics of colossal magneto-resistance (CMR) phenomena has been one of the central issues of condensed matter physics in the last decade. In particular, the ferromagnetic perovskite manganites, e.g., $\text{La}_{1-x}\text{Sr}_x\text{MnO}_3$, have attracted much attention [1]. In these compounds, a $\text{Mn}^{3+}/\text{Mn}^{4+}$ double exchange interaction reduces the transfer energy of the Mn 3d holes through a parallel alignment of neighboring Mn spins [2], resulting in a CMR near the Curie temperature (T_c). In addition, a strong Jahn-Teller effect due to Mn^{3+} leads to the formation of polarons, which strongly affects the transport properties [3]. More recently, the $\text{Tl}_2\text{Mn}_2\text{O}_7$ pyrochlore has been attaining increasing interest, since it exhibits a CMR that is comparable to those observed for the perovskites [4–6]. $\text{Tl}_2\text{Mn}_2\text{O}_7$ is also a ferromagnet, and its resistivity (ρ) drops rapidly upon cooling below $T_c \sim 120$ K. Near and above T_c , an external magnetic field of 7 T reduces ρ by a factor of ~ 10 . Although these features appear very similar to those for the perovskites, various studies have suggested that the underlying mechanism should be very different: In $\text{Tl}_2\text{Mn}_2\text{O}_7$ the electric conduction takes place in a conduction band having strong Tl 6s and O 2p characters, as shown by band calculations [7–9]. The spontaneous magnetization below T_c is produced by the Mn^{4+} sublattice through superexchange interaction, independently from the conduction system. The CMR results from changes in the conduction system caused by the magnetization in the Mn^{4+} sublattice. Little evidence has been found for a double exchange or a Jahn-Teller effect in $\text{Tl}_2\text{Mn}_2\text{O}_7$. Hall ef-

fect experiments [4,10] have shown that the conduction electron density is very low, $n \sim 0.8 \times 10^{19} \text{ cm}^{-3}$ or 0.001 per formula unit (f.u.) above T_c , and that it increases to $n \sim 5 \times 10^{19} \text{ cm}^{-3}$ (0.006 per f.u.) in the ferromagnetic phase. A density increase is also found with applied magnetic field [10]. The carrier density change has been considered a main cause for the CMR in $\text{Tl}_2\text{Mn}_2\text{O}_7$ [10,11].

However, many questions remain regarding the CMR mechanism in $\text{Tl}_2\text{Mn}_2\text{O}_7$. First of all, the microscopic electronic structure of $\text{Tl}_2\text{Mn}_2\text{O}_7$ itself has remained unclear experimentally, since no spectroscopic data have been available, to our knowledge, over a sufficiently wide energy range. Among many other issues, for example, the contribution to the CMR from a change in the carrier mobility, suggested by the much larger variation in ρ than in n [10], has not been studied in detail.

In this work we use optical spectroscopy to probe the microscopic electronic structure of $\text{Tl}_2\text{Mn}_2\text{O}_7$. The optical conductivity $\sigma(\omega)$ of $\text{Tl}_2\text{Mn}_2\text{O}_7$ was obtained from its optical reflectivity $R(\omega)$, measured at photon energies $0.007 \text{ eV} \leq \hbar\omega \leq 30 \text{ eV}$, at temperatures $40 \text{ K} \leq T \leq 300 \text{ K}$, in magnetic fields $B \leq 6 \text{ T}$. Upon cooling through T_c and upon applying B near T_c , $\sigma(\omega)$ indicates a transition from insulatorlike to metallic electronic structures with a large Drude-like component below 0.2 eV. It is found that the B -induced evolution of the electronic structures leading to the CMR is very similar to the T -induced one, and that they are universally related to the macroscopic magnetization. This is the first demonstration of such electronic structures in $\text{Tl}_2\text{Mn}_2\text{O}_7$ as a function of energy. Contributions to the CMR from a change in the carrier mobility are also analyzed.

The $\text{Tl}_2\text{Mn}_2\text{O}_7$ sample used was a polycrystalline disk synthesized by solid state reaction under a pressure of 2 GPa [4]. The measured magnetization of the sample showed a sharp onset at $T_c \sim 120$ K, and near and above T_c the resistivity decreased by a factor of ~ 10 by applying a field of 6 T. These values agree well with those in the literature [4–6,9,10]. The sample surface was mechanically polished for optical studies. Near-normal incidence reflectivity measurements were made using a Fourier interferometer and conventional sources for $\hbar\omega \leq 2.5 \text{ eV}$, and using synchrotron radiation source for $\hbar\omega \leq 30 \text{ eV}$. A gold or a silver film evaporated directly onto the sample surface was used as a reference of the reflectivity below 2.5 eV. The experiments under magnetic fields were done using a superconducting magnet. $\sigma(\omega)$ spectra were obtained from the measured $R(\omega)$ using

the Kramers-Kronig relations [12]. To complete $R(\omega)$, a Hagen-Rubens or a constant extrapolation was used for the lower-energy end, and a ω^{-4} extrapolation for the higher-energy end [12].

Figure 1(a) shows $R(\omega)$ and $\sigma(\omega)$ spectra of $\text{Ti}_2\text{Mn}_2\text{O}_7$ at 295 K up to 30 eV. The spectra are typical of an insulating (semiconducting) oxide, with very small $\sigma(\omega)$ below 1 eV and sharp peaks below 0.1 eV due to optical phonons [15], and indicate a small density of states (DOS) around the Fermi level (E_F). From $\sigma(\omega)$, the band gap of $\text{Ti}_2\text{Mn}_2\text{O}_7$ at 295 K is estimated to be ~ 1.6 eV. The peaks in the spectra above 2 eV can be attributed to charge transfer excitations from O 2p to Mn 3d bands (the strong peak near 2.5 eV) and excitations to other higher-lying states [7–9]. Figure 1(b) shows $R(\omega)$ and $\sigma(\omega)$ below 0.5 eV at several T 's [13]. Upon cooling below $T_c=120$ K, both $R(\omega)$ and $\sigma(\omega)$ increase rapidly, with $R(\omega)$ approaching 1 and $\sigma(\omega)$ showing a sharp rise toward the lower energy end. The emergence of this pronounced Drude-like component clearly demonstrates that the electronic structure near E_F becomes metallic below T_c , with a substantial number of free carriers. The spectral weight of a Drude component in $\sigma(\omega)$ can be related to the effective density of free carriers, N_{eff} , through the optical sum rule [12] as

$$N_{eff} = \frac{n}{m^*} = \frac{2m_0}{\pi e^2} \int_0^{\omega_p} \sigma_D(\omega) d\omega. \quad (1)$$

Here, n is the carrier density, m^* is the effective mass in units of the rest electron mass m_0 , ω_p is the plasma cut-off energy, and $\sigma_D(\omega)$ is the Drude contribution in $\sigma(\omega)$. In the inset of Fig. 1(b) we plot N_{eff} , calculated using (1) as a function of T [14]. Contributions from the phonon peaks in $\sigma(\omega)$ have been subtracted by fitting them with the Lorentz function [12]. The measured low-field magnetization (M) of the sample is also plotted. The increase in N_{eff} is apparently synchronous with that in M below T_c , showing a strong connection between the dynamic charge response and M .

According to the band calculations for ferromagnetic (FM) $\text{Ti}_2\text{Mn}_2\text{O}_7$ [7–9], there is a conduction band with its bottom located ~ 0.5 eV below E_F [9]. This conduction band results from a strong hybridization of Tl 6s, O 2p, and Mn 3d states, and the resulting effective mass is small, $m^* \simeq m_0$. The DOS around E_F is very small, and the calculated electron density is $4 \times 10^{19} \text{ cm}^{-3}$ (0.005 per f.u.). The minimum k -conserving gap in the DOS, which leads to an optical gap in the dipole approximation [12], is 1.5–2 eV in both the majority- and minority-spin band structures. The observed $\sigma(\omega)$ below T_c is consistent with these predictions: In the observed $R(\omega)$ and $\sigma(\omega)$ the metallic components are indeed limited to below 0.5 eV. The onset of $\sigma(\omega)$ was observed at ~ 1.6 eV also below T_c (not shown), similarly to that above T_c shown in Fig. 1. (The spectra above 0.5 eV showed only minor T dependences.) From the measured N_{eff} of 0.01 per f.u. below T_c [see Fig. 1(b)] and the measured density of $n = 0.006$ per f.u. [4,10], we obtain $m^* \sim 0.6m_0$, which is indeed small and close to the calculated m^* .

Hence, the band calculations [7–9] are successful in predicting the basic electronic structures of FM $\text{Ti}_2\text{Mn}_2\text{O}_7$ near E_F .

Figures 2 and 3 show $R(\omega)$ and $\sigma(\omega)$, respectively, in external magnetic fields $B \leq 6$ T, applied normal to the sample surface [16]. The spectral changes at 125 K, near T_c , are quite spectacular: both $R(\omega)$ and $\sigma(\omega)$ show large increases with B , and $\sigma(\omega)$ shows a clear transition from an insulating character at 0 T to a metallic one at 6 T. In contrast, at 160 K and 40 K, away from T_c , they show only small changes. The B -induced spectral changes at 125 K are remarkably similar to those observed with decreasing T at $B=0$ shown in Fig. 1(b). This similarity, emphasized in the bottom graph of Fig. 3, clearly demonstrates that the electronic structures near and above T_c under strong B fields are very similar to those below T_c at $B=0$. Figure 4(a) shows the variation of N_{eff} , calculated with (1), as a function of B relative to that at $B=0$. The relative increase in N_{eff} is largest in the range $120 \text{ K} \leq T \leq 140 \text{ K}$, which is exactly where the measured CMR of the sample was most pronounced.

In Fig. 4(b) we plot N_{eff} as a function of M for different values of T and B [19]. Apparently, N_{eff} has a universal relation with M in quite wide ranges of T and B . The solid curve in Fig. 4(b) is a quadratic fit to the data, which indicates that N_{eff} nearly scales with M^2 . Note that this single universal relation holds in two seemingly distinct regimes, i.e., one below T_c where ρ depends more strongly on T than on B , and the other near and above T_c where ρ depends more strongly on B than on T . This common universal relation, as well as the similarity between T -induced and B -induced spectral changes, indicate that the electronic structures and the dynamic charge response in the presence of a macroscopic magnetization are basically common in the two regimes. Namely, near and above T_c (120 – 140 K), an applied external field aligns the Mn^{4+} spins, which results in polarized band structures and the appearance of a small conduction band, similarly to those below T_c as predicted by the band calculations [7–9]. The CMR in $\text{Ti}_2\text{Mn}_2\text{O}_7$ should be primarily due to this appearance of conduction band in the presence of M induced by external B . This accompanies a large increase in n , as observed by Hall effect [10]. Although a microscopic understanding of the $N_{eff} \propto M^2$ relation is beyond the scope of the present work, it is noteworthy that the measured n has been found to behave as $\propto M^{1.5}$, which can be understood by assuming a linear-in- M shift of a rigid conduction band [10]. Apparently, the B -induced evolution of $\sigma(\omega)$ near T_c can be basically understood with such a shift of conduction band, and with the resulting increase of n .

Regarding the CMR of $\text{Ti}_2\text{Mn}_2\text{O}_7$, as stated before, contributions from changes in m^* and the average scattering time (τ) of the carriers have been unclear. Below we attempt to estimate these contributions using our data. The measured n increases upon cooling through T_c , $n(100 \text{ K})/n(140 \text{ K}) \sim 5$ [10,17]. For $N_{eff} = n/m^*$, this ratio is ~ 8 [see Fig. 1(b)]. These values suggest that

m^* becomes $8/5 \sim 1.5$ times smaller below T_c . From the measured ρ of our sample, the increase in the dc conductivity (σ_{dc}) was $\sigma_{dc}(100 \text{ K})/\sigma_{dc}(140 \text{ K}) \sim 20$. In the Drude theory of metal, $\sigma_{dc} \propto n\tau/m^*$. Comparison with $N_{eff} = n/m^*$ shows that τ becomes $20/8 \sim 2.5$ times longer below T_c . Similar analyses at 140 K on going from $B=0$ to 6 T show that τ becomes longer and m^* becomes smaller, both by a factor of ~ 2 . Hence our estimates suggest that *both τ and m^* vary by a factor of ~ 2 with changing T or B near T_c* . Namely, all of n , τ , and m^* contribute to the CMR in $\text{Ti}_2\text{Mn}_2\text{O}_7$, although n is most significant. Note that the above simple analyses [18] have been possible since the Drude-like component in $\sigma(\omega)$ is completely separated from those due to interband transitions.

Since n is very small above T_c , $\sim 0.8 \times 10^{19} \text{ cm}^{-3}$ [10], a metallic conduction with a well-defined band effective mass is unlikely. Indeed, experimental evidence for a hopping conduction has been reported [11], and a possibility of magnetic polarons has been discussed [20]. Hence the observed decrease of “optical” m^* might be related to a crossover from a hopping-dominated charge dynamics to a Drude-like one. The increase in τ is likely to result mainly from the magnetic critical scattering of carriers by localized spins [21], where the strong spin fluctuations present for $T \geq T_c$ are suppressed for $T < T_c$, leading to larger τ and σ_{dc} . Effects of a local coupling between conduction electrons and Mn spins above T_c have also been discussed [10].

Since different CMR mechanisms have been suggested for pyrochlore $\text{Ti}_2\text{Mn}_2\text{O}_7$ and the perovskite manganites, it is interesting to compare the present results with the optical study of $\text{La}_{1-x}\text{Sr}_x\text{MnO}_3$ (LSMO) [22], a representative CMR perovskite. In $\text{Ti}_2\text{Mn}_2\text{O}_7$, the large T - and B -induced spectral changes are limited to below 0.5 eV, while LSMO shows large variations in $\sigma(\omega)$ over several eV: $\text{Ti}_2\text{Mn}_2\text{O}_7$ involves *an order of magnitude smaller energy scale* than LSMO for the variation of charge dynamics. The small energy scale is closely related with the small n in $\text{Ti}_2\text{Mn}_2\text{O}_7$. Remarkably, $\text{Ti}_2\text{Mn}_2\text{O}_7$ shows a CMR comparable to that for LSMO in spite of this small energy scale and n , due to different characters of the conduction systems. Namely, in $\text{Ti}_2\text{Mn}_2\text{O}_7$ the conduction band has a small m^* resulting from strong Tl 6s and O 2p characters, while in LSMO Mn 3d holes with larger m^* give rise to the conduction. A smaller m^* is more effective in producing a greater variation of σ_{dc} for a given change in n . The spectral changes in the FM phase also have striking qualitative differences: In $\text{Ti}_2\text{Mn}_2\text{O}_7$, the Drude-like spectral component *newly emerges* below T_c in an otherwise insulatorlike spectrum, and the gap itself is almost unchanged. In contrast, LSMO shows a *spectral weight transfer* below T_c from an interband to an intraband component, where their total (combined) N_{eff} appears nearly conserved [22]. This increase in N_{eff} is a unique feature of pyrochlore $\text{Ti}_2\text{Mn}_2\text{O}_7$ that is not observed for the perovskites.

Our $\sigma(\omega)$ data for the CMR pyrochlore $\text{Ti}_2\text{Mn}_2\text{O}_7$

have revealed much new information about its electronic structures as functions of energy, T , and B . With increasing B and with decreasing T near T_c , $\sigma(\omega)$ has shown a dramatic transition from an insulatorlike to a metallic electronic structure. The $\sigma(\omega)$ data show that the B -induced evolution of the electronic structure leading to the CMR is very similar to the T -induced one, and that they are universally related to M in wide ranges of T and B . Our data have also shown that changes in τ and m^* of the carriers also make finite contributions to the CMR. Although the CMR for $\text{Ti}_2\text{Mn}_2\text{O}_7$ appears similar to that for the perovskite manganites, the underlying evolution of charge dynamics in $\text{Ti}_2\text{Mn}_2\text{O}_7$ shown by our work is strikingly different from that reported previously for the perovskites, reflecting different CMR mechanisms in these compounds.

The experiments using synchrotron radiation source was done at the UVSOR Facility, Institute for Molecular Science. We thank the staff for assistance.

- [1] See, for example, Y. Tokura *et al.*, *J. Phys. Soc. Jpn.* **63**, 3931 (1994).
- [2] C. Zener, *Phys. Rev.* **82**, 403 (1951).
- [3] A.J. Millis *et al.*, *Phys. Rev. Lett.* **74**, 5144 (1995).
- [4] Y. Shimakawa *et al.*, *Nature* **379**, 53 (1996); *Phys. Rev. B* **55**, 6399 (1997).
- [5] M.A. Subramanian *et al.*, *Science* **273**, 81 (1996).
- [6] S.-W. Cheong *et al.*, *Solid State Commun.* **98**, 163 (1996).
- [7] D.J. Singh, *Phys. Rev. B* **55**, 313 (1997).
- [8] S.K. Mishra *et al.*, *Phys. Rev. B* **58**, 7585 (1998).
- [9] Y. Shimakawa *et al.*, *Phys. Rev. B* **59**, 1249 (1999).
- [10] H. Imai *et al.*, *Phys. Rev. B* **62**, 12190 (2000).
- [11] B. Martinez *et al.*, *Phys. Rev. Lett.* **83**, 2022 (1999); R. Senis *et al.*, *Phys. Rev. B* **61**, 11637 (2000).
- [12] F. Wooten, *Optical Properties of Solids* (Academic Press, New York, 1972).
- [13] $R(\omega)$ above 2.5 eV was measured at 295 K only, to which $R(\omega)$ below 2.5 eV at lower T 's were smoothly connected.
- [14] We obtained ω_p for each $\sigma(\omega)$ as ω satisfying both $\epsilon_1(\omega)=0$ and $\frac{d\epsilon_1(\omega)}{d\omega} > 0$, where the real dielectric function $\epsilon_1(\omega)$ was calculated from $R(\omega)$ [12].
- [15] N. Massa *et al.*, *Phys. Rev. B* **60**, 7445 (1999).
- [16] $R(\omega)$ in B fields were measured below 0.9 eV only, where $R(\omega)$ showed only minor B -dependence above ~ 0.5 eV.
- [17] The quality of our sample is very similar to that used in Ref. [10], and we have assumed that the carrier densities in the two works are equal.
- [18] Alternatively, we could also estimate τ and m^* as adjustable parameters in fitting $\sigma(\omega)$ to a Drude function. In this treatment the tail of a Drude component contains important information, but this range also contains strong phonon peaks in our data. Consequently we have found that the procedure based on (1) is more plausible than the above one.
- [19] The N_{eff} data at $B=0$ are not included in Fig. 4(b), since we could not accurately measure M at $B=0$ due to magnetic domain effects. M measured at 40 K nearly

saturated above $B \simeq 0.3$ T, hence the N_{eff} data above 0.5 T plotted in Fig. 4(b) are free from magnetic domain effects.

- [20] P. Majumdar and P. Littlewood, Phys. Rev. Lett. **81**, 1314 (1998).
- [21] P.G. de Gennes and J. Friedel, J. Phys. Chem. Solids **4**, 71 (1958); M.E. Fisher and J.S. Langer, Phys. Rev. Lett. **20**, 665 (1968).
- [22] Y. Okimoto *et al.*, Phys. Rev. Lett. **75**, 109 (1995).

FIG. 1. (a) Optical reflectivity (R) and conductivity (σ) of $Tl_2Mn_2O_7$ at 295 K. (b) R and σ measured at different temperatures at zero field. The inset compares the effective carrier density (N_{eff}) and the magnetization (M) at an external magnetic field of 0.2 T, as a function of temperature (T).

FIG. 2. Optical reflectivity (R) of $Tl_2Mn_2O_7$ in magnetic fields at several temperatures.

FIG. 3. Top four graphs: optical conductivity (σ) of $Tl_2Mn_2O_7$ in magnetic fields at several temperatures. Bottom graph: σ at different temperatures and magnetic fields plotted together, demonstrating their similarity (see the text).

FIG. 4. (a) Effective carrier density (N_{eff}) as a function of magnetic field (B), normalized by those at $B=0$. (b) N_{eff} at different temperatures and magnetic fields as a function of magnetization (M). The solid curve is a quadratic fit to the data. The vertical bars indicate N_{eff} arising from the range below 0.007 eV, where the reflectivity spectra were extrapolated.

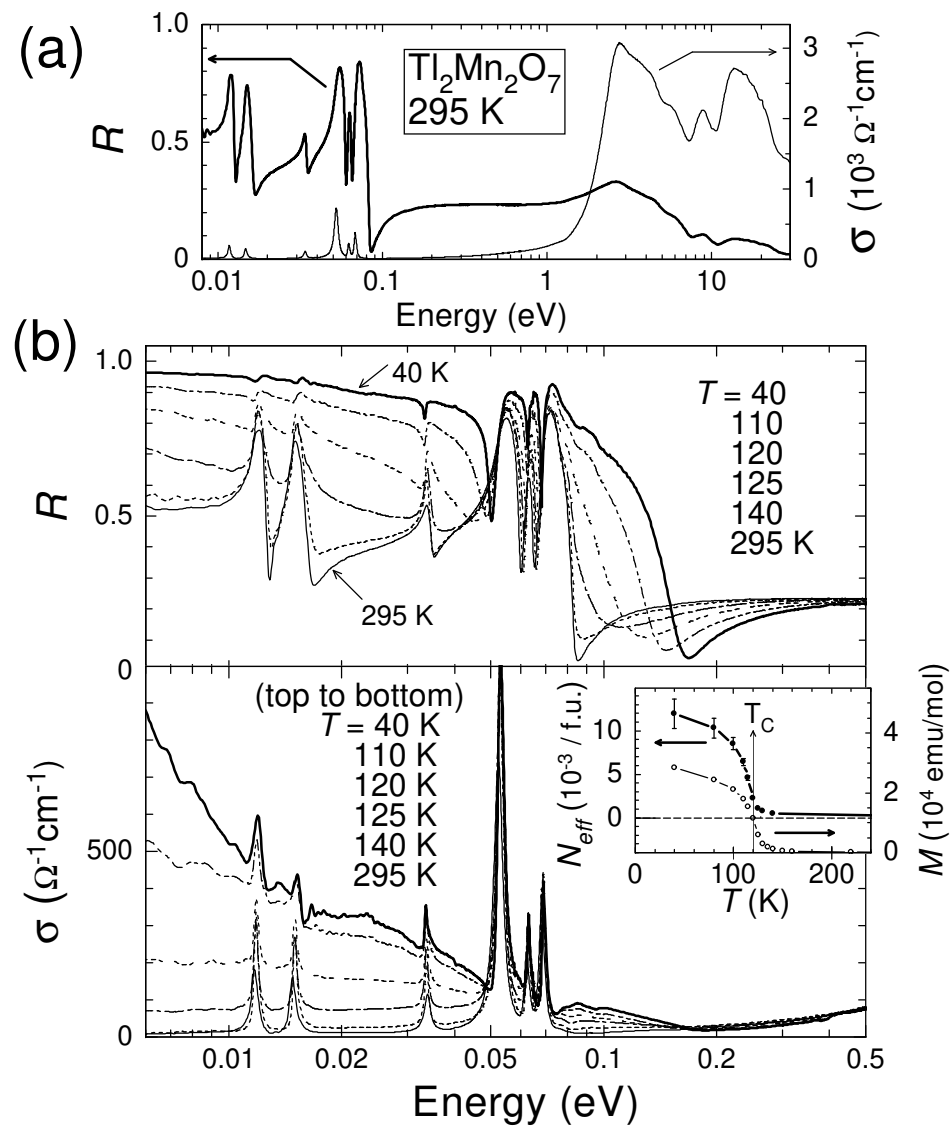


FIG. 1
Okamura et al.

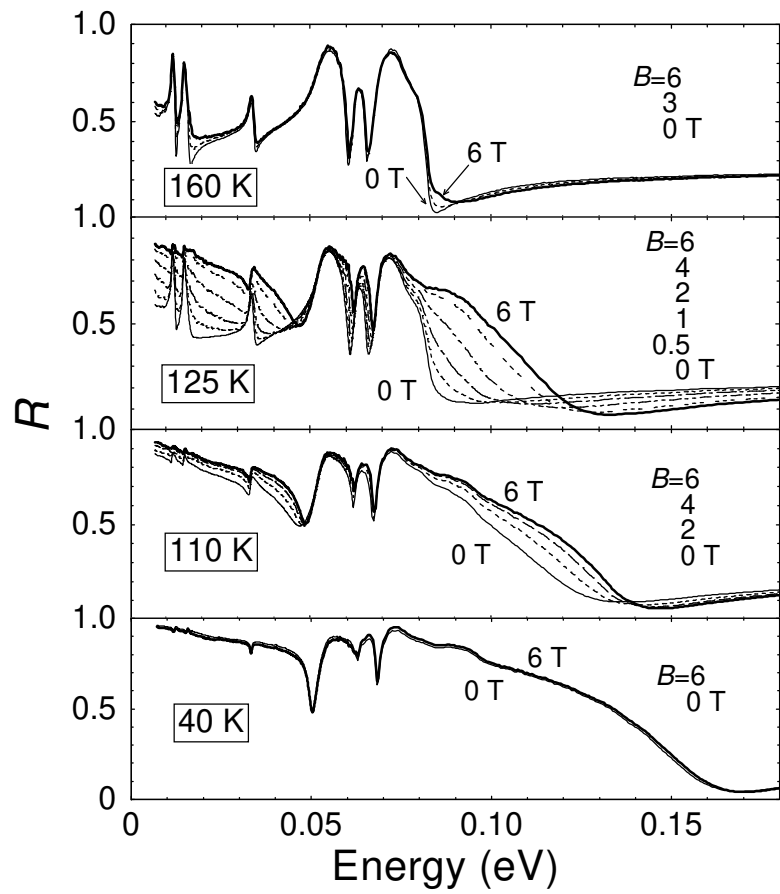


FIG.2
Okamura et al.

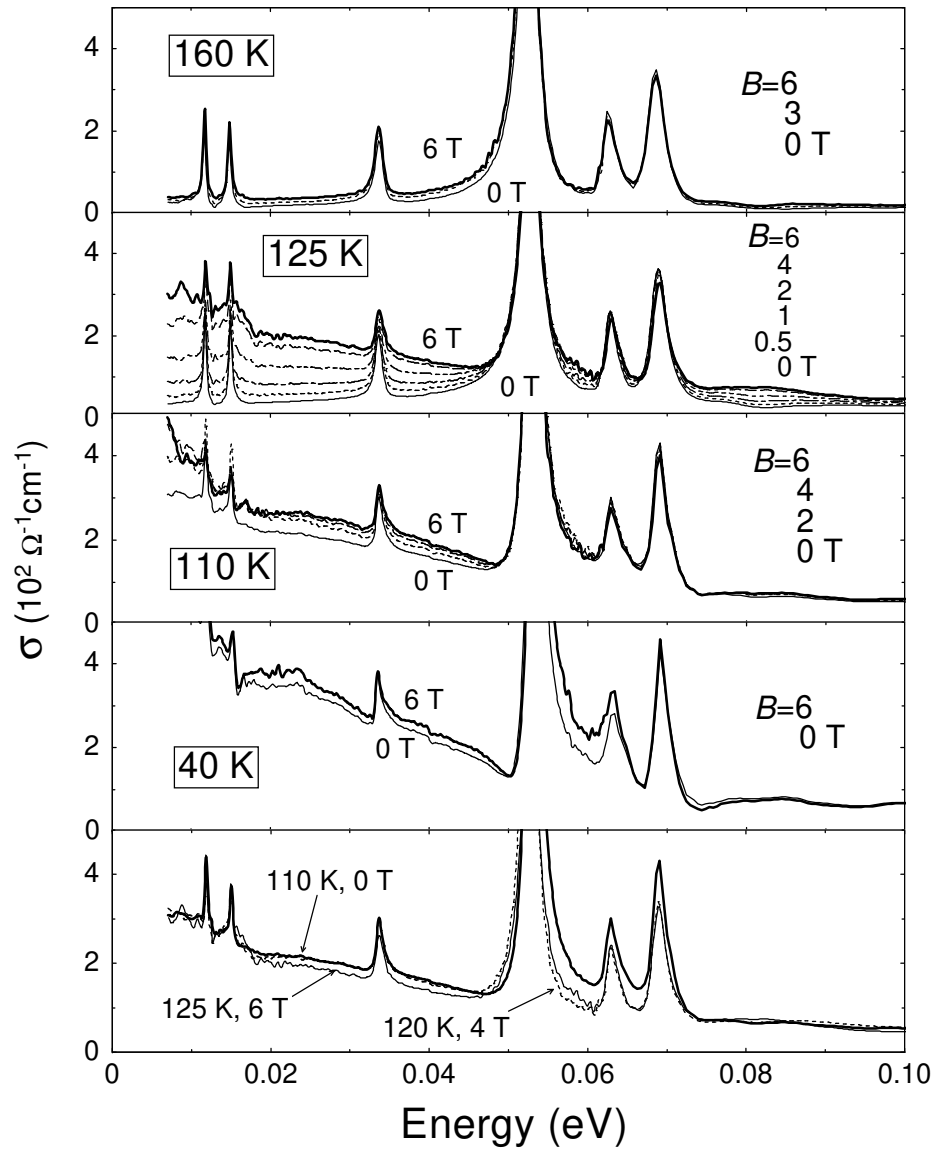


FIG.3
Okamura et al.

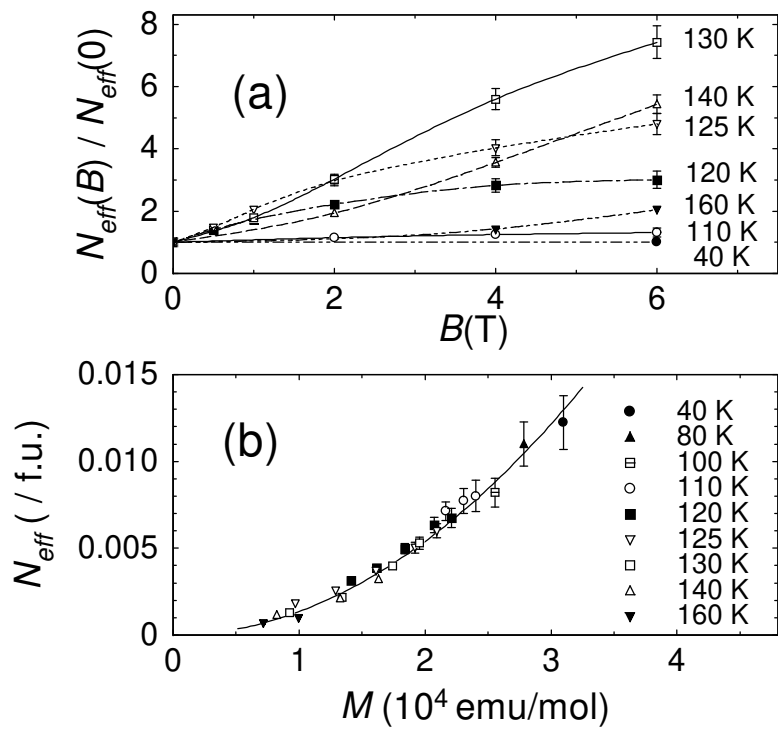


FIG. 4
Okamura et al.

